Inorganic Chemistry

Selective Gas Sorption within a Dynamic Metal-Organic Framework

Banglin Chen,*,[†] Shengqian Ma,[‡] Eric J. Hurtado,[†] Emil B. Lobkovsky,[§] Chengdu Liang,[∥] Haoguo Zhu,[∥] and Sheng Dai[∥]

Department of Chemistry, University of Texas-Pan American, Edinburg, Texas 78541-2999,
Department of Chemistry and Biochemistry, Miami University, Oxford, Ohio 45056,
Department of Chemistry and Chemical Biology, Baker Laboratory, Cornell University,
Ithaca, New York 14853-130, Center for Nanophase Materials Sciences and Chemical
Sciences Divisions, Oak Ridge National Laboratory, Oak Ridge, Tennessee 37831

A microporous metal-organic framework **1** Co(NDC)(4,4′-Bipy)$_{0.5}$·G$_x$ (NDC = 2,6-naphthalenedicarboxylate; 4,4′-Bipy = 4,4′-bipyridine; G = guest molecules) was synthesized and structurally characterized of a doubly interpenetrated primitive cubic net. To make use of the framework flexibility, **1** was activated at temperatures of 150 and 200 °C to form **1a** and **1b**, respectively, exhibiting highly selective sorption behaviors of hydrogen over nitrogen-gas molecules.

Introduction

The last two decades have witnessed rapid progress on microporous metal-organic framework (MOF)[1] materials for their promising applications in gas storage, separation, and heterogeneous catalysis.[2−41] The amenability and extraordinary porosity of such new types of zeolite analogues have not only led to the most-porous materials ever reported for gas storage[2−4] but also initiated the discovery of novel microporous materials for the separation of some specific species such as acetylene.[5−6]

The size-exclusive effects within porous materials have played an important role in their separation functions in which smaller molecules can go through the microporous channels, whereas larger substrates are blocked. In this regard, the emerging microporous MOF materials are of great

---

* To whom correspondence should be addressed. Email: banglin@utpa.edu.
† University of Texas-Pan American.
‡ Miami University.
§ Cornell University.
∥ Oak Ridge National Laboratory.

(1) Eddaoudi, M.; Moler, D. B.; Li, H.; Chen, B.; Reineke, T. M.; O'Keeffe, M.; Yaghi, O. M. *Acc. Chem. Res.* **2001**, *34*, 319. (b) Ferey, G.; Mellot-Draznieks, C.; Serre, C.; Millange, F. *Acc. Chem. Res.* **2005**, *38*, 217. (c) Janiak, C. *Dalton Trans.* **2003**, 2781. (d) Kesanli, B.; Lin, W. *Coord. Chem. Rev.* **2003**, *246*, 305. (e) Kitagawa, S.; Kitaura, R.; Noro, S. *Angew. Chem., Int. Ed.* **2004**, *43*, 2334. (f) Soldatov, D. V.; Ripmeester, J. A. Organic Zeolites. In *Nanoporous Materials IV*; Sayari, A., Jaroniec M., Eds.; Elsevier: Amsterdam, The Netherlands, 2005; pp 37−54. (g) Bradshaw, D.; Claridge, J. B.; Cussen, E. J.; Prior, T. J.; Rosseinsky, M. J. *Acc. Chem. Res.* **2005**, *38*, 273. (h) Lin, W. B. *J. Solid State Chem.* **2005**, *178*, 2486. (i) Rowsell, J. L. C.; Yaghi, O. M. *Angew. Chem., Int. Ed.* **2005**, *44*, 4670.
(2) Rosi, N. L.; Eckert, J.; Eddaoudi, M.; Vodak, D. T.; Kim, J.; O'Keeffe, M.; Yaghi, O. M. *Science* **2003**, *300*, 1127.
(3) Wong-Foy, A. G.; Matzger, A. J.; Yaghi, O. M. *J. Am. Chem. Soc.* **2006**, *128*, 3494.
(4) Férey, G.; Mellot-Draznieks, C.; Serre, C.; Millange, F.; Dutour, J.; Surblé, S.; Margiolaki, I. *Science* **2005**, *309*, 2040.
(5) Matsuda, R.; Kitaura, R.; Kitagawa, S.; Kubota, Y.; Belosludov, R. V.; Kobayashi, R. C.; Sakamoto, H.; Chiba, T.; Takata, M.; Kawazoe, Y.; Mita, Y. *Nature* **2005**, *436*, 238.
(6) Samsonenko, D. G.; Kim, H.; Sun, Y.; Kim, G.-H.; Lee, H.-S.; Kim, K. *Chem.- An Asian J.* **2007**, *1*, 484.
(7) Zhao, X.; Xiao, B.; Fletcher, A. J.; Thomas, K. M.; Bradshaw, D.; Rosseinsky, M. J. *Science* **2004**, *306*, 1012.
(8) Dybtsev, D. N.; Chun, H.; Kim, K. *Angew. Chem., Int. Ed.*, **2004**, *43*, 5033.
(9) Chen, B.; Ockwig, N. W.; Millward, A. R.; Contreras, D. S.; Yaghi, O. M. *Angew. Chem., Int. Ed.* **2005**, *44*, 4745.
(10) Lin, X.; Jia, J.; Zhao, X.; Thomas, K. M.; Blake, A. J.; Walker, G. S.; Champness, N. R.; Hubberstey, P.; Schroder, M. *Angew. Chem., Int. Ed.* **2006**, *45*, 7358.
(11) Sun, D.; Ma, S.; Ke, Y.; Collins, D. J.; Zhou, H.-C. *J. Am. Chem. Soc.* **2006**, *128*, 3896.
(12) Dinca, M.; Dailly, A.; Liu, Y.; Brown, C. M.; Neumann, D. A.; Long, J. R. *J. Am. Chem. Soc.* **2006**, *128*, 16876.
(13) Fang, Q. R.; Zhu, G. S.; Xue, M.; Zhang, Q. L.; Sun, J. Y.; Guo, X. D.; Qiu, S. L.; Xu, S. T.; Wang, P.; Wang, D. J.; Wei, Y. *Chem.− Eur. J.* **2006**, *12*, 3754.
(14) Pan, L.; Adams, K. M.; Hernandez, H. E.; Wang, X.; Zheng, C.; Hattori, Y.; Kaneko, K. *J. Am. Chem. Soc.* **2003**, *125*, 3062.
(15) Dybtsev, D. N.; Chun, H.; Yoon, S. H.; Kim, D.; Kim, K. *J. Am. Chem. Soc.* **2004**, *126*, 32.
(16) Kitaura, R.; Seki, K.; Akiyama, G.; Kitagawa, S. *Angew. Chem., Int. Ed.* **2003**, *42*, 428.
(17) Dinca, M.; Long, J. R. *J. Am. Chem. Soc.* **2005**, *127*, 9376.
(18) Bourrelly, S.; Llewellyn, P. L.; Serre, C.; Millange, F.; Loiseau, T.; Ferey, G. *J. Am. Chem. Soc.* **2005**, *127*, 13519.
(19) Pan, L.; Parker, B.; Huang, X.; Olson, D. H.; Lee, J.; Li, J. *J. Am. Chem. Soc.* **2006**, *128*, 4180.
(20) Navarro, J. A. R.; Barea, E.; Salas, J. M.; Masciocchi, N.; Galli, S.; Sironi, A.; Ania, C. O.; Parra, J. B. *Inorg. Chem.* **2006**, *45*, 2397.

Scheme 1. Schematic Illustration of the Self-assembly of Paddle-wheel Cluster $M_2(CO_2)_4$ with Bicarboxylate $R(COO)_2$ and Bidentate Pillar Linker L to Construct 3D Primitive Cubic MOFs $M(R(COO)_2)(L)_{0.5} \cdot G_x$

Pillared 3D $M(R(COO)_2)L_{0.5}$ bulding block
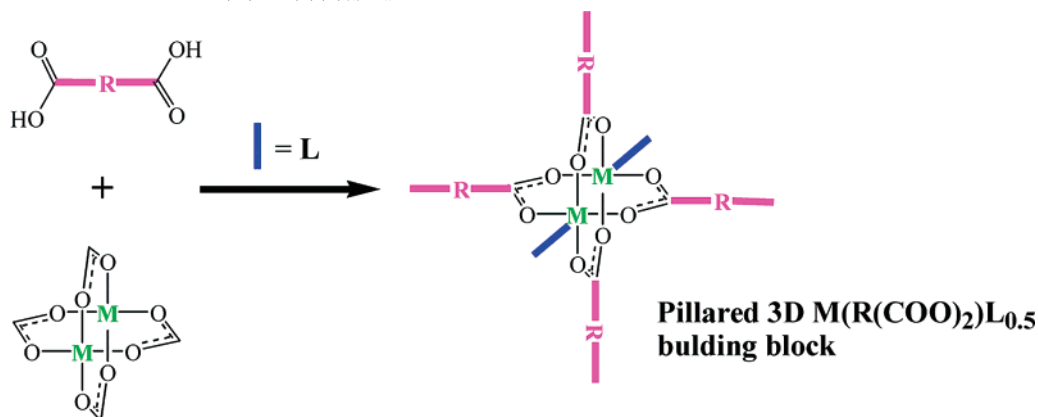
importance because of the tunable and amendable nature of such pores that can be systematically varied by the judicious choice of metal-containing secondary building units (SBUs) and/or bridging organic linkers. Recently, we have been particularly interested in a unique α-Po-type of microporous 3D primitive cubic MOFs $M(R(COO)_2)(L)_{0.5} \cdot G_x$ (M^{2+} = Cu^{2+} and Zn^{2+}, $R(COO)_2$ = bicarboxylate linker, L = bidentate pillar linker, G = guest molecules) to systematically tune the micropores.[27-30] Such 3D primitive cubic MOFs can be easily self-assembled by the paddle-wheel clusters $M_2(CO_2)_4$ with bicarboxylate linker $R(COO)_2$ and bidentate pillar linker L (Scheme 1). It is expected that by the incorporation of different combinations of bicarboxylate $R(COO)_2$ and pillar linker L, a series of microporous MOFs with systematically varied micropores will be readily constructed. The micropores can be further tuned by making use of interpenetration; thus, rationally designed microporous MOFs for highly selective separation and purification of small molecules can be fulfilled. In fact, we have successfully made use of several 3D primitive cubic MOFs Cu(FMA)-$(4,4'$-Bpe$)_{0.5}$,[29] Zn(BDC)$(4,4'$-Bipy$)_{0.5}$,[27] and Zn(BDC)(D-abco)$_{0.5}$[30] (FMA = fumarate, $4,4'$-Bpe = *trans*-bis(4-pyridyl)-

ethylene, BDC = 1,4-benzenedicarboxylate, $4,4'$-Bipy = $4,4'$-bipyridine, Dabco = 1,4-diazabicyclo[2,2,2]octane) to systematically tune their micropores of 2.0×3.2 and 4.0×4.9 Å and intersecting channels of about 7.5×7.5 and 3.8×4.7 Å for their separation of small gas molecules, alkanes, and hexane isomers, respectively.

During the studies on these unique type of microporous MOF materials, a characteristic dynamic feature has been revealed for the doubly interpenetrated MOFs.[16,27-28] As shown in Figure 1, the porous structures of the as-synthesized MOFs can be transformed reversibly into the non- or less-porous structures of the exchanged and/or activated ones that are triggered by guest content and pressure because of their structural flexibility.[27] Although it has been expected that such dynamic features can be specifically utilized for their separation of small molecules by the deliberate control of guest pressure, very few examples of such dynamic MOFs have been realized for such a purpose.[16] Herein, we report a rare example of the dynamic MOF Co(NDC)$(4,4'$-Bipy$)_{0.5} \cdot$(DMF)$_{1.5}$(H$_2$O) (**1**) (NDC = 2,6-naphthalenedicarboxylate; $4,4'$-Bipy = $4,4'$-bipyridine) of two-interpenetrated primitive cubic nets for its selective sorption with respect to H_2 and N_2.

Experimental Section

Materials and Methods: All of the reagents and solvents employed were commercially available and used as supplied without further purification. TGA data were obtained on a TGA G500 V5.3 Build 171 instrument with a heating rate of 5 deg/min under a N_2 atmosphere. Powder XRD patterns were obtained with a Scintag X1 powder diffractometer system, using Kα radiation with a variable divergent slit and a solid-state detector. The routine power was 1400 W (40 kV, 35 mA). Low-background quartz XRD slides (Gem Depot, Inc., Pittsburgh, PA) were used. For analyses, powder samples were dispersed on glass slides.

(21) Rood, J. A.; Noll, B. C.; Henderson, K. W. *Inorg. Chem.* **2006**, *45*, 5521.
(22) Pan, L.; Olson, D. H.; Ciemnolonski, L. R.; Heddy, R.; Li, J. *Angew. Chem.*, *Int. Ed.* **2006**, *45*, 616.
(23) Taylor, T. J.; Bakhmutov, V. I.; Gabbai, F. P. *Angew. Chem.*, *Int. Ed.* **2006**, *45*, 7030.
(24) Humphrey, S. M.; Chang, J.-S.; Jhung, S. H.; Yoon, J. W.; Wood, P. T. *Angew. Chem.*, *Int. Ed.* **2007**, *47*, 272.
(25) Ma, S.; Sun, D.; Wang, X.-S.; Zhou, H.-C. *Angew. Chem.*, *Int. Ed.* **2007**, *46*, 2458.
(26) Maji, T. K.; Matsuda, R.; Kitagawa, S. *Nat. Mater.* **2007**, *6*, 142.
(27) Chen, B.; Liang, C.; Yang, J.; Contreras, D. S.; Clancy, Y. L.; Lobkovsky, E. B.; Yaghi, O. M.; Dai, S. *Angew. Chem.*, *Int. Ed.* **2006**, *45*, 1390.
(28) Chen, B.; Ma, S.; Zapata, F.; Lobkovsky, E. B.; Yang, J. *Inorg. Chem.* **2006**, *45*, 5718.
(29) Chen, B.; Ma, S.; Zapata, F.; Fronczek, F. R.; Lobkovsky, E. B.; Zhou, H.-C. *Inorg. Chem.* **2007**, *46*, 1233.
(30) Bárcia, P. S.; Zapata, F.; Silva, J. A. C.; Rodrigues, A. E.; Chen, B. *J. Phys. Chem. B* **2007**, *111*, 6101.
(31) Seo, J. S.; Whang, D.; Lee, H.; Jun, S. I.; Oh, J.; Jeon, Y. J.; Kim, K. *Nature* **2000**, *404*, 982.
(32) Hu, A.; Ngo, H. L.; Lin, W. *J. Am. Chem. Soc.* **2003**, *125*, 11490.
(33) Seki, K.; Mori, W. *J. Phys. Chem. B* **2002**, *106*, 1380.
(34) Dalai, S.; Mukherjee, P. S.; Zangrando, E.; Lloret, F.; Chaudhuri, N. R. *J. Chem. Soc., Dalton Trans.* **2002**, 822.
(35) Rather, B.; Zaworotko, M. J. *Chem. Commun.* **2003**, 830.

(36) Chun, H.; Dybtsev, D. N.; Kim, H.; Kim, K. *Chem.—Eur. J.* **2005**, *11*, 3521.
(37) Ma, B.-Q.; Mulfort, K. L.; Hupp, J. T. *Inorg. Chem.* **2005**, *44*, 4912.
(38) Choi, E.-Y.; Park, K.; Yang, C.-M.; Kim, H.; Son, J.-H.; Lee, S. W.; Lee, Y. H.; Min, D.; Kwon, Y.-U. *Chem.—Eur. J.* **2004**, *10*, 5535.
(39) Pichon, A.; Fierro, C. M.; Nieuwenhuyzen, M.; James, S. L. *Cryst. Eng. Comm.* **2007**, *9*, 449.
(40) Cho, S.-H.; Ma, B.; Nguyen, S. T.; Hupp, J. T.; Albrecht-Schmitt, T. E. *Chem. Commun.* **2006**, 2563.
(41) Lee, S. W.; Kim, H. J.; Lee, Y. K.; Park, K.; Son, J.-H;, Kwon,Y.-U. *Inorg. Chim. Acta* **2003**, *353*, 151.
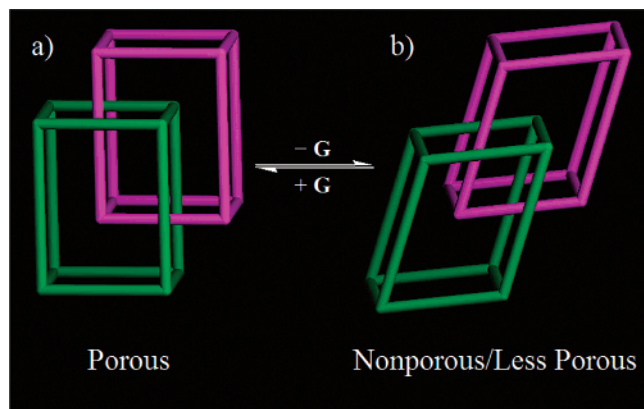
Figure 1. Schematic illustration of the framework transformation between the as-synthesized and the activated MOFs within doubly interpenetrated α-Po nets.

Figure 2. X-ray crystal structure of **1** showing (a) 1D channel of 5.1 × 6.0 Å along the *a* axis and (b) 1D channel of 4.0 × 4.0 Å viewed along the rectangular diagonal of the paddle-wheel clusters.

Synthesis of 1. A mixture of $Co(NO_3)_2 \cdot 6H_2O$ (0.101 g, 0.34 mmol), H_2NDC (0.0747 g, 0.34 mmol), and 4,4′-Bipy (0.0270 g, 0.17 mmol) was suspended in DMF (60 mL) and heated in a vial (60 mL) at 120 °C for 24 h. The dark-orange block-shaped crystals formed were collected, washed with DMF and hexane, and dried in air (0.127 g, 78%). Elemental analysis: Calcd for Co(NDC)-(4,4′-Bipy)$_{0.5}$·(DMF)$_{1.5}$(H$_2$O) ($C_{21.5}H_{22.5}N_{2.5}O_{6.5}Co$): C, 53.92; H, 4.74; N, 7.31; Found: C, 54.09; H, 4.36; N, 7.64.

Single-crystal X-ray Crystallography. Intensity data for the **1** were collected using a Bruker X8 APEX II diffractometer (Mo radiation) in a cold nitrogen stream. Data collection and reduction were done using the Bruker Apex2 software package. Structures were solved by direct methods and refined by full-matrix least-squares, using SHELXL97. All of the non-hydrogen atoms were refined anisotropically. Crystal data for MOF **1**: $Co_2(NDC)_2(4,4′-Bipy) \cdot (G)_x$, triclinic, space group $P(\bar{1})$, $a = 12.939(5)$, $b = 13.092$-(5), $c = 13.754(4)$ Å, $\alpha = 85.449(11)$, $\beta = 70.302(12)$, $\gamma = 83.731(10)°$, $V = 2178.2(13)$ Å^3, $Z = 2$, $D_{calcd} = 1.182$ g cm^{-3}, $\mu = 0.809$ mm^{-1}, $T = 173$ K, R_1 [$I > 2(I)$] $= 0.0524$, wR_2 (all data) $= 0.1377$, $S = 0.951$. **1** is isostructural to Zn(NDC)(4,4′-Bipy)$_{0.5}$.[37]

Gas Sorption Measurements. A Beckman Coulter SA3100 surface area analyzer was used to measure gas adsorption. To remove guest solvent molecules in the framework, the fresh sample soaked in methanol was filtered and vacuumed at 150 °C overnight to form **1a**, and the as-synthesized **1** was filtered and vacuumed at 200 °C overnight to form **1b**. Before the measurement, the sample was vacuumed again using the outgas function of the surface area analyzer for 2 h at 150 °C. A sample of 90.0−100.0 mg was used for sorption measurement and maintained at 77K with liquid nitrogen.

Results and Discussion

1 was synthesized by the solvothermal reaction of H_2NDC, 4,4′-Bipy and $Co(NO_3)_2 \cdot (H_2O)_6$ in *N,N*-dimethylformamide (DMF) at 120 °C for 24 h as dark-orange block-shaped crystals. It was formulated as Co(NDC)(4,4′-Bipy)$_{0.5}$·(DMF)$_{1.5}$-(H$_2$O) by elemental microanalysis and single-crystal X-ray diffraction studies, and the phase purity of the bulk material was independently confirmed by powder X-ray diffraction (PXRD) and thermal gravimetric analysis (TGA).

As expected, the framework is composed of paddle-wheel dinuclear Co$_2$ units, which are bridged by NDC dianions and further pillared by 4,4′-bipyridine to form a 3D two-

interpenetrated elongated primitive cubic (α-Po) structure. Because of double interpenetration of the 3D frameworks, the pores within **1** are reduced to be of ca. 5.1 × 6.0 Å along the *a* axis (part a of Figure 2) and of ca. 4.0 × 4.0 Å along the rectangular diagonal of the paddle-wheel clusters (part b of Figure 2). The bicarboxylate linker NDC in **1** is longer than BDC in Zn(BDC)(4,4′-Bipy)$_{0.5}$, whereas the pillar linker 4,4′-Bipy in **1** is shorter than 4,4′-Bpe in Zn(NDC)(4,4′-Bpe)$_{0.5}$, thus the accessible volume of 42% in **1** is between 28% in Zn(BDC)(4,4′-Bipy)$_{0.5}$ and 56% in Zn(NDC)(4,4′-Bpe)$_{0.5}$.[27−28]
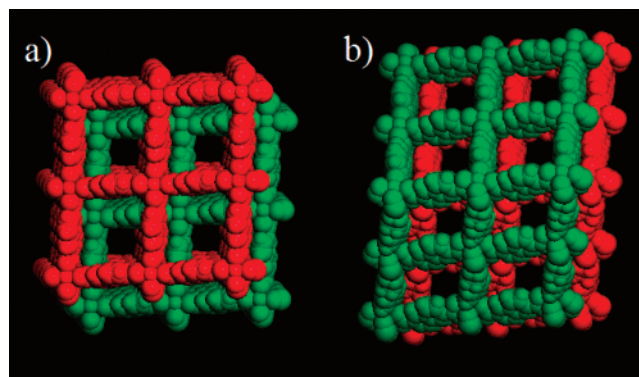
Because there exist no specific interactions between the two interpenetrated frameworks, **1** was expected to exhibit a dynamic feature involving framework transformations/deformations, as revealed in MOFs Zn(BDC)(4,4′-Bipy)$_{0.5}$ and Zn(NDC)(4,4′-Bpe)$_{0.5}$.[27−28] Immersing the as-synthesized **1** in pure methanol slightly led to the reduced d spacing of the structure as shown in methanol-exchanged PXRD pattern (parts a and b Figure 3), which was systematically right-shifted. Such a change of PXRD patterns might be attributed to the guest-induced framework transformations because of the shifting of the frameworks, thus the pore space for the encapsulation of solvent molecules in methanol-exchanged **1** is reduced compared with the as-synthesized **1**. The shifting of the frameworks within dynamic doubly interpenetrated MOFs has been well established by Kitagawa et al.[1e] Although we have not been able to systematically index these patterns and thus rationalize their framework shrink in detail because of the low-resolved PXRD patterns, TGA studies on the as-synthesized and methanol-exchanged **1** have exclusively established that the methanol-exchanged **1** is less porous than the as-synthesized **1**, thus the as-synthesized **1** liberated more guest molecules (part b of Figure 3, black) than methanol-exchanged **1** (part b of Figure 3, red).

To examine permanent porosity and thus to establish the feasibility of **1** for selective gas sorption, methanol-exchanged **1** was activated at 150 °C under a vacuum overnight to get **1a** for gas sorption studies. As revealed in its PXRD, **1a** is a crystalline MOF (part a of Figure 3, green). It needs to be mentioned that methanol-exchanged **1** can be easily regenerated by immersing **1a** into methanol (part a of Figure 3, blue), indicating that the framework transformation between methanol-exchanged **1** and activated **1a** is reversible.

(a)

(b)
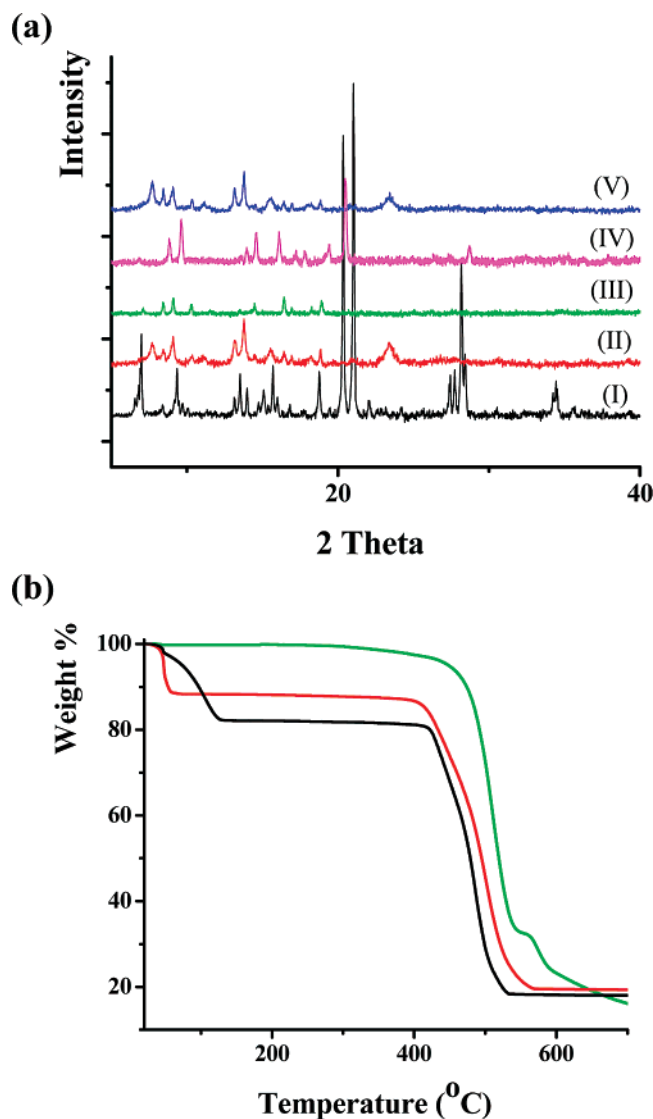
Figure 3. (a) XPRD patterns of as-synthesized ((I), black) and methanol-exchanged ((II), red) **1**, activated **1a** ((III), green) and **1b** ((IV), magenta), and methanol-regenerated ((V), blue) **1′**, and (b) TGA traces of as-synthesized ((I), black) and methanol-exchanged ((II), red) **1**, and activated **1a**.

(a)

(b)

Figure 4. Gas sorption isotherms of (a) **1a** and (b) **1b** at 77 K (H_2, green; N_2, blue).

The N_2 sorption isotherm (part a of Figure 4) shows typical Type I sorption behavior for **1a** with a Langmuir surface area of 115 m^2/g and a pore volume of 0.10 cm^3/g, which are comparable with those reported in Zn(NDC)(4,4′-Bipy)$_{0.5}$.[37] This surface area is significantly low for such a highly porous crystal structure and is only about one-eighth of 946 m^2/g for Zn(BDC)(4,4′-Bipy)$_{0.5}$[27] and less than half of 303 m^2/g for Zn(NDC)(4,4′-Bpe)$_{0.5}$.[28] Most interesting of all, **1a** takes up more H_2 than N_2, which might be utilized for the separation of H_2/N_2. The hydrogen uptake is about two times higher than the nitrogen uptake around P/P_o of 0.5. Its hydrogen storage capacity is about 0.72 wt % at 1 atm. Such preferential hydrogen uptake over nitrogen might be attributed to multidimensional micropores in which some of them are accessible to hydrogen but not to nitrogen.

The porosity of activated **1** is presumably dependent on the activation profile because of the dynamic nature of the framework; thus, the as-synthesized **1** was activated at a higher-temperature of 200 °C under a vacuum overnight to form **1b**. To our surprise, such high-temperature activation even formed a better high-crystalline material **1b** (Figure 3, magenta). The PXRD peaks of **1b** are slightly right-shifted with respect to **1a**, indicating that **1b** might have even smaller micropores and thus take up less hydrogen than **1a**. Most important of all, the smaller micropores within **1b** are generally not accessible to nitrogen at low pressure, thus the capacities of **1b** for the H_2/N_2 separation are significantly enhanced with a hydrogen uptake of about nine times higher than nitrogen around P/P_o of 0.5.

The richness of paddle-wheel clusters $M_2(COO)_4$ has allowed us to assemble a series of α-Po-type 3D primitive cubic MOFs $M(R(COO)_2)(L)_{0.5} \cdot G_x$ in which Zn^{2+} and Cu^{2+} have been widely incorporated.[27−30,33−40] Co^{2+} and Ni^{2+} have been rarely assembled into paddle-wheel clusters for the construction of such α-Po-type MOFs. The only reported MOFs are triply interpenetrated Co(NDC)(4,4′-Bipy)$_{0.5}$ and Ni(NDC)(4,4′-Bipy)$_{0.5}$ that were synthesized by hydrothermal reactions.[41] The higher-temperature reactions for the construction of these two MOFs are mainly responsible for their high-fold framework interpenetration, leading to the formation of nonporous MOFs. By simply making use of DMF as

the solvent at a moderate temperature of 120 °C, we have been able to construct a doubly interpenetrated **1** that is porous. Reaction temperature does play an important role to control the framework interpenetration. It is of interest to note that the doubly and triply interpenetrated Zn(NDC)-(4,4′-Bipy)$_{0.5}$ can be readily synthesized in DMF at temperatures of 80 and 120 °C, respectively.[36−37]

The nature of framework flexibility and robustness is dependent on a lot of subtle factors including the rigidity of metal-containing SBUs and organic linkers, interactions between the frameworks themselves, and interactions between the frameworks and guest molecules.[1e] For specific types of the interpenetrated primitive cubic (α-Po) nets constructed from the paddle-wheel dinuclear M2 units that are bridged by bicarboxylate dianions and pillared by bidentate organic linkers, the shorter and more-rigid bicarboxylates and organic linkers are expected to enforce framework robustness and thus to accelerate the framework transformation in which the activated, and thus compressed, frameworks can be more easily transformed back to open frameworks, as shown in Zn(BDC)(4,4′-Bipy)$_{0.5}$.[27] The instant transformation between dense and open frameworks in Zn(BDC)(4,4′-Bipy)$_{0.5}$ has led to its much-higher porosity than those more-flexible frameworks Co(NDC)(4,4′-Bipy)$_{0.5}$ (**1**) and Zn(NDC)(4,4′-Bpe)$_{0.5}$,[28] although the last two have structurally more accessible void volumes. Without the specific interactions between the interpenetrated frameworks to enforce framework robustness, it is expected that the longer bicarboxylates and more-flexible bidentate organic linkers will lead to more flexible frameworks. Although such framework flexibility is not beneficial to fully make use of the structurally accessible void space for gas storage at low pressure, it might be useful for their potential applications in gas separation as revealed in **1a** and **1b**. It is of interest to note that the recently reported Cu(BPDC)(4,4′-Bipy)$_{0.5}$ (BPDC = 4,4′-biphenyldicarboxylate) exhibits high framework robustness with respect to high-temperature activation.[39] The richness of bicarboxylates and bidentate organic linkers to construct such simple cubic (α-Po) nets of diverse flexibility and robustness will be expected to produce a variety of microporous MOFs for their potential applications in gas storage and separation.

Supporting Information Available: X-ray data of **1** in CIF format. This material is available free of charge via the Internet at http://pubs.acs.org.

IC7013573